Stability Characteristics of Linear Unstable Modes in Flow Past Elliptic Cylinders

Deepak Kumar and Bhaskar Kumar

Abstract Linear stability analysis of steady two-dimensional flow past elliptic cylinders with different aspect ratios (Ar) has been conducted for Reynolds number (Re) up to 200. The main characteristics of the steady flow (bubble length, bubble width, drag coefficient, and maximum vorticity on the cylinder surface) have been presented. From the linear stability computations, we find that there are three sets of complex eigenmodes which become unstable with increasing Re. We refer to them as primary wake mode (PWM), secondary wake mode, and tertiary wake mode (TWM), respectively. PWM and SWM have already been reported in the literature for flow past a circular cylinder. In this work, we report a new unstable mode (TWM) along with PWM and SWM in the wake of elliptic cylinders. The structure of TWM shows that it is not so prominent in the near wake but has the longest range of presence and extends all the way up to the downstream boundary. The critical Re for the onset of instability of these modes and the corresponding Strouhal number (St) have been computed. Least-square fit equations for critical Re and St as a function of Ar have also been presented.

Keywords Steady flow · Linear stability analysis · Elliptic cylinders

Nomenclature

a	Semi-major axis [m]
b	Semi-minor axis [m]
Ar	Aspect ratio [−]
H	Computational domain half width [−]
L_B	Bubble length [−]

D. Kumar (✉)
Department of Mechanical Engineering, NIT Durgapur, Durgapur 713209, India
e-mail: dkumar.me@nitdgp.ac.in

B. Kumar
Department of Mechanical Engineering, IIT Guwahati, Guwahati 781039, India

K. M. Singh et al. (eds.), *Fluid Mechanics and Fluid Power, Volume 2*, Lecture Notes in Mechanical Engineering, https://doi.org/10.1007/978-981-99-5752-1_25

W_B	Bubble width [−]
C_D	Drag coefficient [−]
ω_{max}	Maximum vorticity on the cylinder surface [−]
Re	Reynolds number [−]
St	Strouhal number [−]
λ_r	Growth rate [−]
PWM	Primary wake mode [−]
SWM	Secondary wake mode [−]
TWM	Tertiary wake mode [−]

1 Introduction

Bluff body wakes have been of interest in fluid mechanics since a long time. Flow past an elliptic cylinder is the generalization of flow past a circular cylinder which involves a new variable: the aspect ratio (Ar). In the past, there have been several attempts to investigate this flow [5, 12–14, 20, 24, 26]. The dynamics of the wake of an elliptic cylinder is much more rich compared to the same for a circular cylinder. As we change the aspect ratio of the cylinder, the flow becomes more and more complex. For example, flow past an elliptic cylinder is characterized by the presence of a near wake vortex street (von Kármán vortex street) followed by the diffusion of vortices to form two parallel shear layers. As we go downstream in the wake, the oscillations in the shear layers intensify, finally causing the secondary vortex street to develop [19]. With a decrease in aspect ratio, the extent of the von Kármán vortex street reduces in the wake and the onset location of the secondary vortex street moves close to the cylinder. For low aspect ratios, the shedding pattern is very complex and chaotic with the appearance of vortex pairing and long wavelength wake oscillations [24].

The flow transition between steady to unsteady occurs at Re which depends on Ar of the cylinder. Several researchers [12, 17, 24] in the past have conducted linear stability analysis of steady flow past elliptic cylinders in order to investigate the transition phenomenon. Based on such studies, it is known that the cause and appearance of the Kármán vortex street could be related to the first instability of the wake. The first instability of the wake is related to the growth of the unstable mode, sometimes referred to as the Kármán mode. In the present work, we refer to it as PWM. This is therefore seen as the fundamental cause of unsteadiness in the flow. In the literature, the nature and characteristics of this mode is known for more than forty years. For flow past a circular cylinder, Barkley and Henderson [2] concluded that there is only one mode which becomes unstable leading to the primary wake instability in a two-dimensional flow before the three-dimensionality appears. In contrast, Boppana and Gajjar [3] reported the presence of a second unstable mode before the onset of three-dimensionality. We refer this mode as SWM. According to them, the second unstable mode loses stability somewhere between Re = 125 and 150. In the same year, Verma

and Mittal [25] conducted a linear stability investigation of two-dimensional flow past a circular cylinder. They reported Re = 110.8 for the onset of instability of the SWM. They found that structure of SWM is very similar to PWM. However, SWM has a lower growth rate and higher St than PWM.

In this work, we share the discovery of yet another mode which is unstable in flow past elliptic cylinders, apart from the two already known. We refer this new mode as TWM. Knowledge of the nature and characteristics of these modes is of great relevance in understanding the wake flows. The present work examines the characteristics of these modes. We conduct this study for varying Ar of the cylinder and different Re in the range 30–200.

2 Methodology

The governing equations for the fluid flow are the incompressible form of the Navier–Stokes equations. In this work, we use the stabilized finite element formulation to solve the Navier–Stokes equations as well as the eigenvalue problems emanating from the linear stability equations. The stabilized finite element (streamline-upwind/Petrov–Galerkin and pressure-stabilizing/Petrov–Galerkin) method has been developed and used by several researchers in the past [4, 10, 11, 16, 23]. Mittal and Kumar [16] briefly describe the formulation and the numerical method employed here.

Applying the finite element formulation to linear stability equations leads to a generalized matrix eigenvalue problem, and its solution results in the eigenpair. Since the numerical dimension of the problem is usually very large, we look for the few modes which have the largest real part.

Figure 1 illustrates the flow configuration, the computational domain, as well as the boundary conditions. The elliptic cylinder is placed symmetrically in a rectangular domain with its major axis ($2a$) aligned with the flow direction. The cylinder center is considered the origin of the Cartesian coordinate system. Semi-major axis of the ellipse is taken as the length scale for presenting the results. The length of the minor axis is denoted by $2b$, and b/a represents Ar of the cylinder. Nine different Ar values (= 1, 0.75, 0.5, 0.375, 0.25, 0.125, 0.0625, 0.03, 0.01) are used in this study. In the present work, the domain boundaries are located far enough so that there is no significant effect on the overall flow field. The distance of the downstream, the upstream, and the cross-stream boundaries are 700, 200, and 100 from the center of the cylinder. The finite element mesh employed in this work contains 249,165 nodes and 247,654 elements in the computational domain. Close to the cylinder surface and in the wake region, the mesh is kept fine enough to capture the separating shear layer, the boundary layer, the wake bubble of the steady flow, and the linear stability modes accurately. In the direction away from the cylinder, the mesh gradually becomes coarser. The details about the finite element mesh can be found in our recent article [15].

The following boundary conditions are used to compute the steady base flow. The velocity at the upstream boundary is given a free-stream value. In the downstream

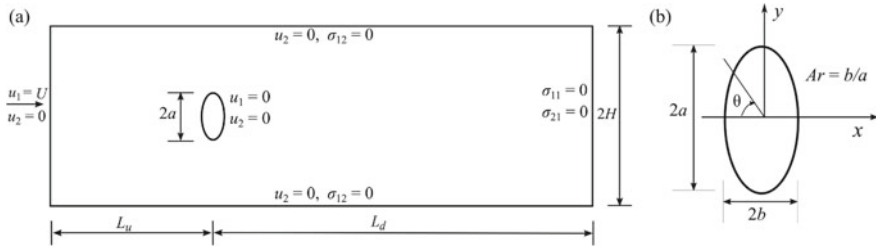

Fig. 1 Problem description: **a** computational domain and boundary conditions, where L_d and L_u represent the downstream and upstream boundaries location, and H denotes the half width of the cross-stream dimension. **b** elliptic cylinder geometry. The cylinder center is used as an origin to measure all the linear distances

boundary, a boundary condition of Neumann type is imposed on the velocity, which corresponds to a zero stress vector. The components of velocity normal to and stress vector along the lower and upper boundaries are assigned zero values. The cylinder surface is a no-slip boundary. Linear stability computations are based on the same boundary conditions except at the inflow border, where the velocity components are set to zero.

The mesh convergence study is comprehensively discussed in one of our recent publications. Tables I and II of Kumar and Kumar [15] provide a detailed discussion of the mesh convergence study, and based on these results, it can be safely concluded that the mesh considered here is appropriate for performing the present study. Tables III and IV of Kumar and Kumar [15] compare the steady flow characteristics with the published data. The comparison reveals that the present results match very well with the earlier investigations on flow past elliptic cylinders.

3 Results and Discussion

3.1 Steady Flow Results

Here, we display results for steady flow past elliptic cylinders for (nine) different Ar and for Re in the range 30–200. As of now, it is well established that, beyond a particular Re, the flow separates from the cylinder surface [5, 20], which causes the formation of the wake bubble. Figure 2 demonstrates the description of the separation wake bubble. The bubble length (L_B) is characterized as the distance between the rear stagnation point and the wake stagnation point along the wake centerline of the cylinder. The bubble width (W_B) is measured as the maximum distance between the lower and upper separation streamlines.

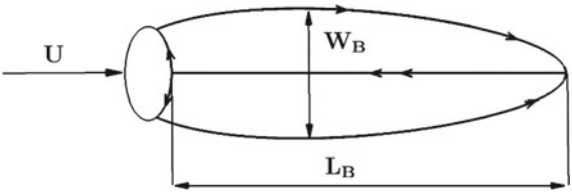

Fig. 2 Description of the symmetric wake bubble: L_B denotes the bubble length, while W_B represents the bubble width

$$\left.\begin{aligned} L_B &= -0.7155 + 0.1301\mathrm{Re} \\ W_B &= 0.4788 + 0.2444\mathrm{Re}^{0.5} \\ C_D &= 0.2938 + 7.6937\mathrm{Re}^{-0.5} \\ \omega_{\max} &= -2.9870 + 2.3980\mathrm{Re}^{0.35} \end{aligned}\right\} \quad (1)$$

Figure 3 displays the variation of the bubble parameters with Ar and Re. For each Ar, it has been found that L_B grows practically linearly as Re increases. The decrease in Ar causes bubble to substantially grow. A non-linear growth is observed for W_B as Re increases while Ar decreases. The drag coefficient (C_D) shows a monotonic decrease with increase in Re and Ar. The maximum vorticity on the cylinder surface ($\omega_{\max}$) increases with decrease in Ar and increase in Re. The least-square fit of the steady flow data shown in Fig. 3 indicates that for Ar = 1.0, L_B, W_B, $\omega_{\max}$, and C_D vary linearly as a function of Re, $\mathrm{Re}^{0.5}$, $\mathrm{Re}^{0.35}$, and $\mathrm{Re}^{-0.5}$, respectively. These results agree with the characteristics of steady flow past a circular cylinder reported by several investigators in the past [6–8, 21, 22]. Theoretical study by Smith [22] showed that L_B grows linearly with Re while W_B increases like $O(\mathrm{Re}^{1/2})$. Fornberg [6] calculated the steady flow numerically up to Re = 600. He observed that L_B increases linearly with Re, whereas W_B grows as $O(\mathrm{Re}^{1/2})$ up to Re = 300 and increases linearly after that. Recently, Sen et al. [21] reported the empirical relations for steady flow past Ar = 1.0 at low Re in the range 6–40. They found that L_B, C_D, and $\omega_{\max}$ vary with Reynolds number as Re, $\mathrm{Re}^{-0.5}$, and $\mathrm{Re}^{0.5}$, respectively. The variation of $\omega_{\max}$ is accurate for low Re. For Re > 30, we find $\mathrm{Re}^{0.35}$ gives better results.

The empirical equations obtained for the curve fit for Ar = 1.0 are given in Eq. 1 for Re in the range 30–200. In general, with the decrease in Ar, it is observed that, the characteristics of the wake bubble vary in the same fashion as for Ar = 1.0, except that a higher-order polynomial fit is required. This shows that the non-linearity in the bubble properties increases with decrease in Ar. However, C_D is one exception to this change. It shows linear variation with $\mathrm{Re}^{-0.5}$ even for smaller aspect ratios. The maximum percentage error between the actual value and the data obtained from the given equations are 0.88 for L_B, 2.22 for W_B, 0.31 for C_D, and 0.53 for $\omega_{\max}$. The trends represented by the equations therefore are a good representation of the variation of the flow properties.

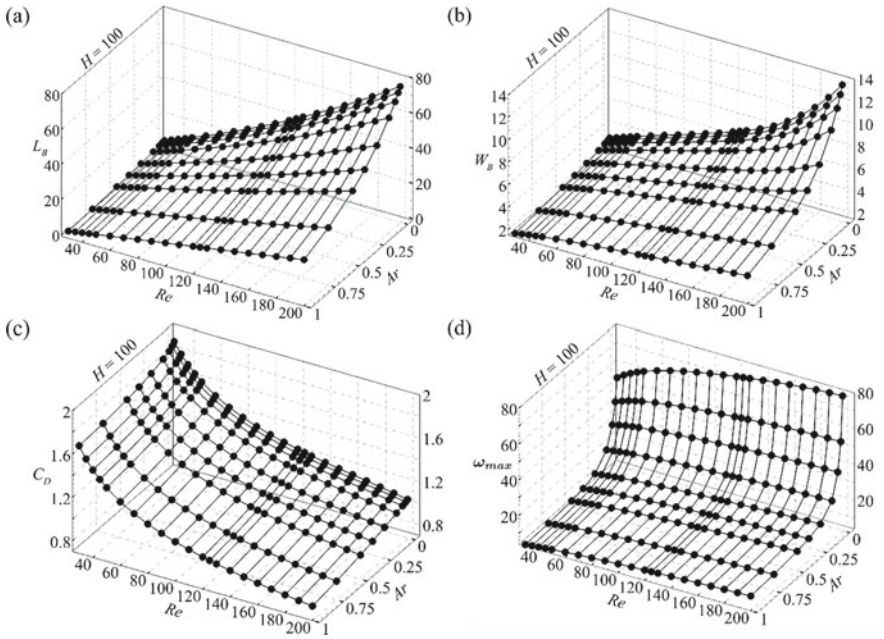

Fig. 3 Steady flow characteristics: effect of Re and Ar on **a** L_B, **b** W_B, **c** C_D, **d** $\omega_{\max}$ on the cylinder surface

4 Linear Stability Analysis

In the past, linear stability analysis of flow past an elliptic cylinder has been carried out by several researchers [12, 17, 24]. However, the results are very scanty and do not give a comprehensive view of the flow behavior. Here, we provide a detailed analysis of the related flow problem. The linear stability study is carried out for cylinders with different Ar and different flow Re. Our results show the presence of three different kinds of eigenmodes in the flow which become unstable with increase in Reynolds number. We refer to them as PWM, SWM, and TWM. These are identified based on their growth rate and modal structure in the flow field. The growth rate (λ_r) of PWM is the highest. It loses stability at relatively low Re and is responsible for shedding of von Kármán vortices. Upon increasing the Re further, first the SWM and then the TWM loses stability. However, TWM is not observed to become unstable for Ar = 0.75 and 1.0.

The parameters like Ar and Re significantly affect the flow behavior, and hence, their effect is studied in more detail. Figure 4 illustrates the variation of λ_r and St with Re for PWM, SWM, and TWM. For PWM, the λ_r curves for Ar = 1.0 and 0.75 show a monotonic increase with Re. For other aspect ratios, it first increases and then passes through a maximum. It is found from these results that flow past a cylinder with low Ar exhibits higher growth rate at lower Re. Consequently, the critical Reynolds

number (Re_c) for the onset of vortex shedding decreases for cylinder with smaller Ar [13, 24]. Similar observations can be made for SWM and TWM. For SWM, the λ_r curve for Ar = 1.0, 0.75, and 0.5 increases monotonically with Re. For other aspect ratios, it shows a non-monotonic increase passing through a maximum. For TWM, the monotonic increase in λ_r is observed for Ar down to 0.25. Below this, the non-monotonic increase similar to that found with the other modes is observed. For the considered Re range, TWM remains stable for Ar = 1.0 and 0.75. It becomes marginally unstable for Ar = 0.5 at Re = 200. And for lower Ar, it becomes unstable over a range of Re. Bottom row of Fig. 4 displays the variation of St with Re for the three modes. For PWM, St curves show a non-monotonic variation for higher aspect ratio cylinders (Ar = 1.0, 0.75, 0.5). Similar observation has been reported for Ar = 1.0 by several researchers in the past [1, 9, 18]. For lower Ar, St of PWM shows a non-monotonic decrease with increase in Re. SWM and TWM exhibit a monotonic decrease in St with increase in Re, for each Ar. There is however one difference in the St curves for TWM. Overall, the slope of the St curves, for TWM, is smaller than the other two modes, and therefore, the minimum which they reach, in the range of Re shown, is higher than that achieved by the other two modes.

We determine the critical parameters (Re_c and St_c) for PWM, SWM, and TWM, corresponding to their zero growth rate.

Figures 5 and 6 show that the value of Re_c and St_c for each eigenmode decreases as we decrease the cylinder aspect ratio. The possible reason for the decrease in Re_c is because the flow past a cylinder with low Ar exhibits higher growth rate at lower Re (see Fig. 4). Our calculations show that TWM does not become unstable for Ar = 1.0 and 0.75 below Re = 200. Thompson et al. [24] performed linear stability analysis of flow past elliptic cylinders with varying Ar. The critical parameters reported in their work for the onset of instability correspond to the same for PWM in our case. For Ar = 1.0, 0.75, 0.5, and 0.25, they reported Re_c value as 47.2, 42.6, 38.8, and 35.6, respectively. In the present study, we find Re_c value for Ar = 1.0, 0.75, 0.5, and 0.25 as 46.9, 42.1, 38.3, and 35.1, respectively. Similarly, they reported the corresponding

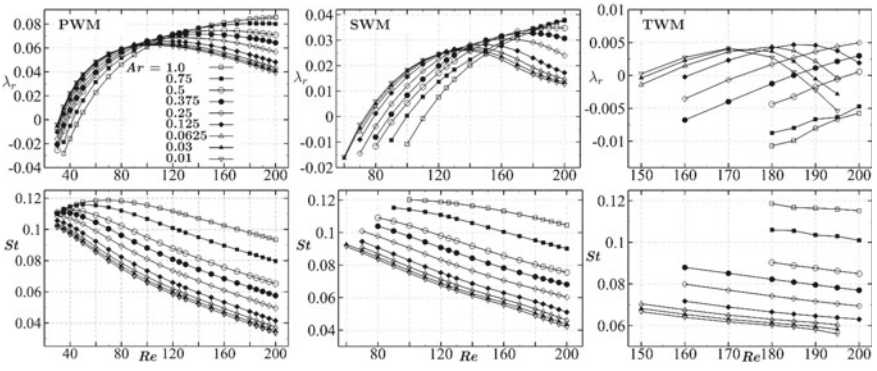

Fig. 4 Variation of λ_r (top) and St (bottom) of PWM (left), SWM (middle), and TWM (right) with increasing Re for different Ar

St_c value for Ar = 1.0, 0.75, 0.5, and 0.25 as 0.1163, 0.1144, 0.1120, and 0.1074, respectively. We find St_c for the same values of Ar as 0.1167, 0.1150, 0.1126, and 0.1082, respectively. The comparison shows that the results are in agreement.

The work done by Boppana and Gajjar [3] on flow past a cascade of circular cylinder showed the presence of second unstable pair (SWM in the present nomenclature) which becomes unstable between Re = 125 and 150. The critical value was however not reported. Verma and Mittal [25] were the first to determine Re_c value for the SWM for flow past a circular cylinder. Re_c value reported by them is 110.8 and St_c though not mentioned explicitly is close to 0.12. The data presented in Fig. 5 depict a close match with these results. The difference in Re_c value with the prediction of Boppana and Gajjar [3] could be attributed to the use of different lateral width of the domain. Table 1 gives the least-square curve fit equations for Re_c and St_c as a function of Ar. The maximum percentage error between the data obtained from the

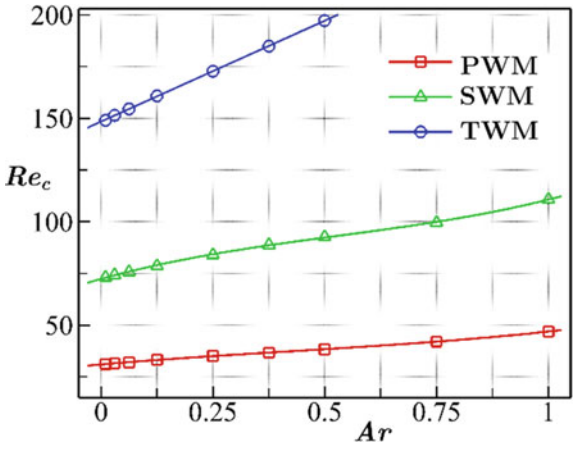

Fig. 5 Variation of Re_c with Ar for PWM, SWM, and TWM

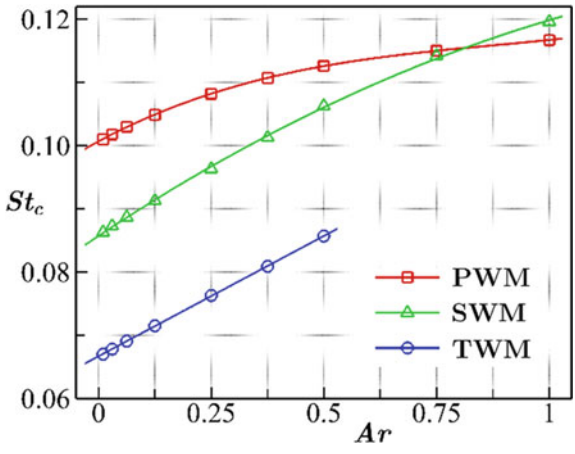

Fig. 6 Variation of St_c with Ar for PWM, SWM, and TWM

given equations of Re_c and the actual value are 0.26 for PWM, 0.47 for SWM, and 0.19 for TWM.

Similarly for St_c, the maximum percentage errors are 0.07 for PWM, 0.41 for SWM, and 0.12 for TWM.

Figure 7 presents the vorticity field for the real parts of PWM, SWM, and TWM for flow past a cylinder with Ar = 0.25 at Re = 180. The mode structures shown are typical and are observed to have similar features at other Reynolds numbers as well. The vorticity field of these modes is symmetric about the wake centerline. This is opposite to that of the base flow. From the figure, we can see that the strength and extent of the three modes vary in the flow field. Here, it should be noted that the range of the vorticity was kept same for all plots. PWM appears more prominent in the near wake and decays rapidly as we move downstream. Comparatively, SWM extends to a much larger distance away from the cylinder. Its strength seems to increase as we move downstream; however, there is a decrease in strength in the far wake. TWM is not so prominent in the near wake, but has the longest range of presence and extends all the way up to the downstream boundary. In general, it is found that the modes with larger growth rates come close to the cylinder and are shorter in their streamwise length compared to the modes which have lower growth rates. In other words, stronger modes tend to approach the cylinder and also contract, whereas the modes which are weaker tend to recede and elongate. Also, the size of the vortical structure in the modes decreases with increase in their oscillation frequency. These observations are in agreement with the wide range of calculations which we have conducted and can also be seen to agree with the images shown in Fig. 7.

Table 1 Least-square fit equations for Re_c and St_c for PWM, SWM, and TWM, obtained as a function of Ar

	Re_c	St_c
PWM	$10.2144\,Ar^3 - 13.0845Ar^2 + 18.7881Ar + 31.0082$	$0.0131\,Ar^3 - 0.0352\,Ar^2 + 0.0381\,Ar + 0.1007$
SWM	$37.3984\,Ar^3 - 59.4328\,Ar^2 + 60.3704\,Ar + 72.3436$	$-0.0131\,Ar^2 + 0.0472\,Ar + 0.0857$
TWM	$97.5631Ar + 148.410$	$0.0381\,Ar + 0.0667$

For PWM and SWM, $0.01 \leq Ar \leq 1.0$ and for TWM, $0.01 \leq Ar \leq 0.5$

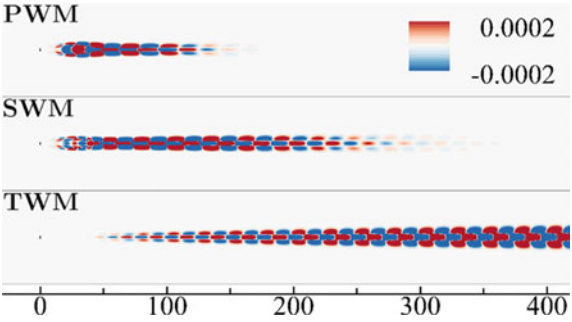

Fig. 7 Structure of the eigenmodes: vorticity fields (real parts) of PWM, SWM, and TWM obtained for Re = 180 flow past a cylinder with Ar = 0.25

5 Conclusion

The linear stability analysis of two-dimensional steady base flow past elliptic cylinders of varying aspect ratios ($0.01 \leq \text{Ar} \leq 1.0$) and Reynolds number ($30 \leq \text{Re} \leq 200$) has been investigated. The steady flow parameters, like L_B, W_B, $\omega_{\max}$ on the cylinder surface, and C_D, have been presented, and their trends are discussed. Linear stability analysis of steady flow past elliptic cylinders yields the presence of three different eigenmodes (PWM, SWM, and TWM). It is observed that these modes show a non-monotonic variation of growth rate with Re for low Ar cylinders. This may also be true for higher Ar cylinders for a larger range of Re. Low Ar cylinders exhibit higher growth rate at lower Re. As a result, Re_c value for the onset of vortex shedding decreases for smaller Ar. For PWM, the variation of St with Re is non-monotonic for higher Ar. For SWM and TWM, St decreases monotonically with Re for all Ar. An interesting correlation exists between the structure of the eigenmodes and their growth rate and St. Modes which have larger growth rate reach close to the cylinder surface and have comparatively shorter length in the wake. Additionally, the size of the vortical structures present in a mode is large if its St is small and vice versa. The difference in the structure of PWM, SWM, and TWM among themselves can be related to the corresponding change in their growth rate and St.

References

1. Barkley D (2006) Linear analysis of the cylinder wake mean flow. Europhys Lett 75:750
2. Barkley D, Henderson RD (1996) Three-dimensional floquet stability analysis of the wake of a circular cylinder. J Fluid Mech 322:215–241
3. Boppana VBL, Gajjar JSB (2011) Onset of global instability in the flow past a circular cylinder cascade. J Fluid Mech 668:304–334
4. Brooks AN, Hughes TJR (1982) Streamline upwind/petrovgalerkin formulations for convection dominated flows with particular emphasis on the incompressible Navier Stokes equations. Comput Methods Appl Mech Eng 32:199–259
5. Dennis SCR, Young PJS (2003) Steady flow past an elliptic cylinder inclined to the stream. J Eng Math 47:101–120

6. Fornberg B (1985) Steady viscous flow past a circular cylinder up toReynolds number 600. J Comput Phys 61:297–320
7. Fornberg B (1991) Steady incompressible flow past a row of circular cylinders. J Fluid Mech 225:655–671
8. Gajjar JSB, Azzam NA (2004) Numerical solution of the Navier-Stokes equations for the flow in a cylinder cascade. J Fluid Mech 520:51–82
9. Giannetti F, Luchini P (2007) Structural sensitivity of the first instability of the cylinder wake. J Fluid Mech 581:167–197
10. Hughes TJR, Brooks AN (1979) A multidimensional upwind scheme with no crosswind diffusion. In: Finite element methods for convection dominated flows, Hughes TJR (ed). ASME, pp 19–35
11. Hughes TJR, Franca LP, Balestra M (1986) A new finite element formulation for computational fluid dynamics: V. circumventing the babuŝka-brezzi condition: a stable petrov-galerkin formulation of the stokes problem accommodating equal-order interpolations. Comput Methods Appl Mech Eng 59:85–99
12. Jackson CP (1987) A finite-element study of the onset of vortex shedding in flow past variously shaped bodies. J Fluid Mech 182:23–45
13. Johnson SA, Thompson MC, Hourigan K (2001) Flow past elliptical cylinders at low Reynolds numbers. In: Proceedings of 14th Australian fluid mechanics conference. Adelaide, pp 343–346
14. Johnson SA, Thompson MC, Hourigan K (2004) Predicted low frequency structures in the wake of elliptical cylinders. Eur J Mech (B/Fluids) 23:229–239
15. Kumar D, Kumar B (2022) Steady flow past elliptic cylinders with blockage effects. Phys Fluids 34(5):053606
16. Mittal S, Kumar B (2003) Flow past a rotating cylinder. J Fluid Mech 476:303–334
17. Paul I, Prakash KA, Vengadesan S (2014) Onset of laminar separation and vortex shedding in flow past unconfined elliptic cylinders. Phys Fluids 26:023601
18. Pier B (2002) On the frequency selection of finite-amplitude vortex shedding in the cylinder wake. J Fluid Mech 458:407–417
19. Pulletikurthi V, Paul I, Prakash KA, Prasad B (2019) On the development of low frequency structures in near and far laminar wakes. Phys Fluids 31:023604
20. Sen S, Mittal S, Biswas G (2012) Steady separated flow past elliptic cylinders using a stabilized finite-element method. Comput Model Eng Sci 86:1–27
21. Sen S, Mittal S, Biswas G (2009) Steady separated flow past a circular cylinder at low Reynolds numbers. J Fluid Mech 620:89–119
22. Smith FT (1979) Laminar flow of an incompressible fluid past a bluff body: the separation, reattachment, eddy properties and drag. J Fluid Mech 92:171–205
23. Tezduyar TE, Mittal S, Ray SE, Shih R (1992) Incompressible flow computations with stabilized bilinear and linear equal-orderinterpolation velocity-pressure elements. Comput Methods Appl Mech Eng 95:221–242
24. Thompson MC, Radi A, Rao A, Sheridan J, Hourigan K (2014) Low-Reynolds-number wakes of elliptical cylinders: from the circular cylinder to the normal flat plate. J Fluid Mech 751:570–600
25. Verma A, Mittal S (2011) A new unstable mode in the wake of a circular cylinder. Phys Fluids 23:121701
26. Yoon HS, Yin J, Choi C, Balachandar S, Ha MY (2016) Bifurcation of laminar flow around an elliptic cylinder at incidence for low Reynolds numbers. Prog Comput Fluid Dyn 16:163–178